RESEARCH ARTICLE

Urban VOC profiles, possible sources, and its role in ozone formation for a summer campaign over Xi'an, China

Jian Sun[1,2] · Zhenxing Shen[2] · Yue Zhang[2] · Zhou Zhang[3] · Qian Zhang[2] · Tian Zhang[2] · Xinyi Niu[4] · Yu Huang[5] · Long Cui[5] · Hongmei Xu[2] · Hongxia Liu[2] · Junji Cao[5] · Xuxiang Li[1]

Abstract

To insight the urban volatile organic compound (VOC) profiles and its contribution to ozone, four-time per day (8:00–9:00, 15:00–16:00, 19:00–20:00, and 23:00–24:00) off-line VOC samples were collected from 16th July to 28th July 2018 for a summer investigation campaign over Xi'an, China. The diurnal variation was significant that the lowest TVOC concentrations were observed in the midnight period (28.4 ± 25.6 ppbv) while the highest was shown in the morning (49.6 ± 40.1 ppbv). The differences of total non-methane VOCs (TVOCs) between weekdays and weekend were also significant that the weekend showed significantly high VOC levels than weekdays ($p < 0.05$) but did not lead to significant ambient O_3 increase ($p > 0.05$). Isopentane, a general marker for vehicle exhaust, showed descending concentrations from morning to midnight and good correlation with vehicle numbers on road, indicating a potential source to the VOCs at this site. The results from PMF proved that vehicular exhaust was the largest source to the VOCs in this study (64.4%). VOC categories showed a reverse sequence in abundance of concentrations and OFP contributions that alkenes showed the highest OFPs although with the lowest abundance in TOVCs due to their high reactivity in photochemical reactions. High OFPs from ethylene and isopentane indicated that vehicular emissions could be the largest potential OFP source in this site. OFPs from isoprene (from 1.85 to 13.4 ppbv) indicated that biogenic VOCs should not be negligible in urban Xi'an city when controlling O_3 pollutants. Comparison of two OFP methods was conducted and MIR method was proved to be more reasonable and scientific in summer Xi'an. Therefore, vehicular emission, the largest contributor to ambient VOCs and also OFPs, as well as biological source should be priority controlled in guiding VOC emissions and reducing O_3 control policies.

Keywords VOC profiles · OFP · Temporal variation · Source apportionment

Introduction

As one of the fastest-growing economies (over 7% annual GDP growth for the past 20 years) (NBSC 2018), China is now suffering serious environmental pollution issues (Cai et al. 2010; Cao et al. 2012). In recent years, episodes of ozone (O_3) concentrations exceeding 120 ppbv occur frequently during summer time especially in megacities such as Beijing,

✉ Zhenxing Shen
zxshen@mail.xjtu.edu.cn

[1] School of Human Settlements and Civil Engineering, Xi'an Jiaotong University, Xi'an 710049, China

[2] Department of Environmental Science and Engineering, Xi'an Jiaotong University, Xi'an 710049, China

[3] Changsha Center for Mineral Resources Exploration, Guangzhou Institute of Geochemistry, Chinese Academy of Sciences, Changsha, China

[4] The Jockey Club School of Public Health and Primary Care, The Chinese University of Hong Kong, Hong Kong, China

[5] Key Lab of Aerosol Chemistry & Physics, Institute of Earth Environment, Chinese Academy of Sciences, Xi'an 710049, China

Shanghai, Guangzhou, and Xi'an (Shen et al. 2016; Tan et al. 2018; Li et al. 2019). Better understanding of the causes of elevated ozone in China is important for developing effective emission control strategies.

VOCs are widely known as precursors of ozone in the presence of nitrogen oxides (NO_x) and sunlight (Kumar et al. 2017; Li et al. 2017). It has been widely proved that the photochemical reactions of VOCs play an important role in the formation of ground-level O_3 (Duan et al. 2008; Li et al. 2017; Wang et al. 2017). United States Environmental Protection Agency (USEPA) has particularly defined 57 VOC species as critical ozone precursors to in controlling O_3 problem (Shao et al. 2016; USEPA 1998). Additionally, some VOC species such as benzene, toluene, and 1,3-butadiene have been evidenced to be air toxics for their adverse effects on human health (Kampa and Castanas 2008).

Emissions of large amount of anthropogenic VOCs are prevalent in urban areas due to the large number of vehicles and massive industries (Hwa et al. 2002; Lee et al. 2002). Consequently, the VOCs in urban atmosphere maintained at very high level in these years (Hui et al. 2018; Yuan et al. 2013) Li et al., 2015. Numerous studies indicated that the composition of atmospheric VOCs in urban area was complex and derived from multiple sources, including vehicle exhaust, petrochemical industry emissions, fossil fuel volatilization, the use of chemical solvents (i.e., coating, painting, etc.), and biomass combustion (An et al. 2017; Tan et al. 2018; Xue et al. 2017)Kountouriotis et al., 2014. However, significant variations were existed between VOC compositions and sources in different regions. Zou et al. (2015) reported that aromatic hydrocarbons contributed 35% to total non-methane hydrocarbons in Beijing but as high as 54% in Guangzhou. The results in Zhang et al. (2016) showed that aromatic hydrocarbons in northern China were affected mainly by biomass/biofuel/coal burning, whereas sites in southern China were affected mainly by traffic-related emissions and/or industrial emissions.

Previous researches on VOCs in China mostly focused on developed regions, such as Beijing-Tianjin-Hebei region, Yangtze River Delta, and Pearl River Delta (Duan et al. 2008; Wang et al. 2018; Yuan et al. 2010). Very few studies were conducted in Guanzhong Plain although the air quality there was one of the most severe regions and at the same time being the largest economic output in Northwest China (Xu et al. 2018). Xi'an, as the center city of Guanzhong Urban Agglomeration and listed as top ten megacities in China, has over 8 million population and 2.5 million vehicles (SPBS 2017). Xi'an has been long suffered from serious air pollution (Shen et al. 2008, 2009, 2010, 2011, 2016); in summer, O_3 was regarded as the primary pollutant in 70% of polluted cases (Sun et al. 2019; Wang et al. 2012). According to the Chinese National Monitoring Station, the 90% percentile of monthly average O_3_8h concentrations in 2017 and 2018 summer were both over 200 $\mu g\ m^{-3}$, which was exceeding the national

standards (GB3095-2012). However, researches on ambient VOCs and their source apportionment are rare, leading to many O_3 modeling studies still using outdated VOC data (Feng et al. 2016; Li et al. 2018). The crowed transportation and booming industry (including automobile, petroleum chemical, textile, manufacturing, and power plant) in Xi'an collectively emitted a large number of VOCs to the atmosphere. Some VOC source profiles have been reported in literature including vehicle exhaust and biomass burning, but owing to the limited VOC source apportionment results, O_3 pollutant control during summer time was inefficient in recent years (Cheng et al. 2018).

In this study, the ambient VOCs at a typical sampling station in Xi'an were monitored from 16th July to 28th July 2018 using modified SUMMA canister method. Four samples per day make it possible to get diurnal variations of VOCs. The objectives of this study are to (1) detect the contribution of ambient VOCs on ground O_3 in Xi'an during summer time and (2) identify the potential sources of ambient VOCs during summer time in Xi'an, China. This study would provide an up-to-date ambient VOC data to relevant modeling researches and facilitate the government in formulating efficient O_3 control policies.

Methodology

Sample collection

Field VOC samples were collected from 16th July 2018 to 28th July 2018, when O_3 episodes happened the most frequently led by the specific weather conditions, on the roof of a 15-m high building located in the southeastern part of downtown Xi'an (Fig. S1 in Supplementary Material). The north and east sides to the sampling site are residential areas and the campus of Xi'an Jiaotong University, and the south is about 100 m away from the South Second Ring Road and west sides are another main roads of Xi'an City. There are no factories nor workshops near the sampling site; thus, it is suitable for monitoring typical urban VOCs in ambient air (Shen et al. 2008; Shen et al. 2010; Shen et al. 2009; Zhang et al. 2015).

The ambient air samples were collected four times per day during the sampling period, namely 8:00–9:00, 15:00–16:00, 19:00–20:00, and 23:00–24:00. Reasons for the timing of sampling were illustrated in Section S1 (Supplementary Material). Ambient air was compressed into clean evacuated 3 L silonite-treated stainless steel canisters (Entech Instruments Inc., Simi Valley, California, USA) to approximately 100 KPa in 60 min controlled by a flow controller at a constant flow rate of 50 mL/min. A total of 56 samples were obtained during the 2-week strengthened study. Along with the VOC sample collection, continuous measurement of gaseous pollutants (CO, O_3, SO_2, and NO_x) was conducted as

well. The instruments used for gaseous pollutant monitoring are shown in Table S1 (Supplementary Material).

Laboratory analysis of VOCs

Analysis of the VOC samples was entrusted by Institute of Geochemistry, Chinese Academy of Sciences. The air samples were analyzed with a model 7200 preconcentrator (Entech Instruments Inc., California, USA) coupled with an Agilent 5977 gas chromatography mass selective detector/flame ionization detector (GC-MSD/FID, Agilent Technologies, USA). Detailed information about the analysis method was described in Zhang et al. (2016). In summary, 500 mL air samples were drawn from the canister through a liquid nitrogen-cooled cryogenic trap (0.32 cm × 20 cm) with glass beads (60/80 mesh) at − 160 °C. After trapping, this primary trap was heated to 10 °C, and all target compounds were transferred using pure helium as mobile phase to the secondary trap (0.32 cm × 20 cm) at − 50 °C with Tenax-TA (60/80 mesh) as adsorbents. This micropurge-and-trap step could remove mostly of the redundant H_2O and CO_2 in air sample. The secondary trap was then heated to get VOCs transferred by helium to a third cryofocus trap (0.08 cm × 5 cm) at − 170 °C. After the focusing step, the trap was rapidly heated and the VOCs were transferred to the GC-MSD/FID system. The mixture was first separated by a DB-1 capillary column (60 m × 0.32 mm × 1.0 μm, Agilent Technologies, USA), with helium as the carrier gas at a constant rate of 4.0 mL/min, and then split into two ways controlled by a splitter to a 0.35 m × 0.10 mm I.D. stainless steel line output to MSD detection, and to a HP PLOT-Q column (30 m × 0.32 mm × 20.0 μm, Agilent Technologies, USA) output to flame ionization detector (FID) detection. The GC oven temperature was programmed to be initially at 10 °C, held for 3 min; this then increased to 120 °C at 5 °C/min, and then to 250 °C at 10 °C/min with a final hold time of 20 min. The MSD was operated in selected ion monitoring mode and the ionization method was electron impacting (EI, 70 eV). A total of 106 VOC species were measured in this study and the minimum detection limits (MDLs) are shown in Table S2. The MDLs for 106 VOC species ranged from 4 to 181 pptv and 101 of them were lower than 100 pptv.

Ozone formation potential calculation

As many VOCs are well-known O_3 precursors in the atmosphere (Wang et al. 2017), ozone formation potential (OFP) was calculated in this study to estimate the contribution from photochemical reactions of VOCs. One method was maximum incremental reactivity (MIR) (Carter 2009), which was shown in Eq. (1).

$$OFP_i = [VOC_i] \times MIR_i, \tag{1}$$

where OFP_i, $[VOC_i]$, and MIR_i are the ozone formation potential and are the concentration and maximum incremental reactivity of individual VOC_i, respectively. In Carter's study, the MIR model required a VOC-limited and high NO_x condition which applied to the Guanzhong area (Li et al. 2017; Xue et al. 2017; Zhang et al. 2015).

Another method was propene-equivalent (Prop-Equiv) concentration (Atkinson and Arey 2003), calculated as Eq. (2)

$$Prop-Equiv_i = [VOC_i] \times k_{OH,i}/k_{OH,propene}, \tag{2}$$

where $K_{OH,i}$ and $K_{OH,propene}$ are the rate constants of VOC_i and propene reacted with OH at 298 K, respectively. The values of MIR and K_{OH} are summarized in Table S3.

Source apportionment model

Positive matrix factorization (PMF) model was widely used in VOC source apportionment studies (An et al. 2017; Duan et al. 2008; Guo et al. 2011; Shao et al. 2016). US EPA PMF 5.0 model was employed in the present study. The function of the PMF model is to identify the number of emission sources and the species profile of each source, and to attribute the amount of mass from each source to each species in each individual sample by an analyst based on the measured data at the receptor site (Guo et al. 2011). Based on the data matrix X of i by j dimensions (i means number of samples and j means VOC species measured), the calculation principle could be presented by the equation as Eq. (3):

$$x_{ij} = \sum_{k=1}^{p} g_{ik} f_{kj} + e_{ij} \tag{3}$$

where x_{ij} is the jth species concentration measured in the ith sample, g_{ik} is the species contribution of the kth source to the ith sample, f_{kj} is the jth species fraction from the kth source, e_{ij} is the residual for each sample/species, and p is the total number of independent sources (Shao et al. 2016). Uncertainty level was necessary in PMF model and for species with concentration higher than MDL, the uncertainty levels could be calculated by Eq. (4), otherwise by Eq. (5):

$$Uncertainty = \sqrt{(EF \times Concentration)^2 + MDL^2} \tag{4}$$

$$Uncertainty = \frac{5}{6} \times MDL \tag{5}$$

where MDL represents the minimum detection limit (as an absolute concentration value) and the EF for the relative measurement error determined by calibration of the instruments (as 15% in this study).

In this study, although 106 species were measured and 86 of them were quantified, it was not necessary to use all of them for the PMF model. Referring to principles from EPA PMF Model 5.0 (http://www.epa.gov/heasd/research/pmf.html), the

unique VOC species that are important tracers of sources, such as isoprene, were selected in model calculation in this study. Table S4 shows that the VOC species selected were appropriate for source apportionment in this study.

Results and discussion

General description of VOC level over Xi'an

The statistical results of 106 measured VOCs during the sampling period are shown in Table 1 (data of 22th July was absent due to electricity problem). Overall, 86 out of the 106 species were measured with concentrations over detect limitations. The daily concentrations of TVOC (86 species with concentrations over MDL) were 42.6 ± 45.8 ($24.3 – 61.4$) ppbv. The lowest TVOC concentrations were observed in the night period ($23:00 – 24:00$, 28.4 ± 25.6 ppbv) which may be due to the lowest anthropogenic activity level (Li et al. 2017). By contrast, the highest TVOC concentration was shown in the morning (49.6 ± 40.1 ppbv). Compared with TVOC concentrations in megacities with severe O_3 population in China, Xi'an has been faced the VOC-related air pollution issue as severe as Beijing (48.9 ppbv), Shanghai (37.5 ppbv), and Guangzhou (39.7 ppbv) (Han et al. 2017; Zhang et al. 2018; Zou et al. 2015). While compared with Tokyo (27.4 ppbv) and Seoul (35.6 ppbv) which have successively controlled O_3 problem (Hoshi et al. 2008; Huang et al. 2015; Song et al. 2019), there should be a hard and long way for Xi'an in VOCs and O_3 control.

The 86 measured VOCs were classified into 7 categories and the distributions are shown in Fig. S2. OVOCs were the biggest contributor to TVOCs with daily average proportion of 37%. As a crucial production of photochemical reactions in atmosphere, the high compositions of OVOCs during summer time in Xi'an were reasonable (Louie et al. 2013). Followed by OVOCs, alkanes and halocarbons were another two crucial compositions with occupation of 27% and 17%, respectively. Aromatics and alkenes showed comparable contributions to TVOCs (7%). Acetylene contributed as much as 4% to TVOC alone; however, the occupation of carbon disulfide was negligible (< 1%).

The most abundant VOC in this study was acetone, followed by ethane and isopentane, with the daily average concentrations of 11.9 ± 8.44, 1.97 ± 1.17, and 1.87 ± 2.06 ppbv, respectively. Generally, short-chain hydrocarbons (i.e., acetylene, ethylene, and ethane), halocarbons (i.e., chloromethane), and OVOCs (i.e., acetone) were comparable abundant among the VOC species. These short-chain VOCs were widely reported to be derived from biomass and biofuel burning (An et al. 2017; Guo et al. 2011). At the same time, benzene and isopentane were also abundant which were highly correlated with vehicular emissions (Hwa et al. 2002). The solvent-

originated compounds (i.e., toluene and m/p-xylene) also showed relative high concentrations (Kumar et al. 2018; Yurdakul et al. 2018). This characteristic in VOC compositions indicated that the atmospheric VOCs in urban Xi'an were determined by a combined influence from complex sources.

Diurnal variation of VOCs and trace gas

Diurnal and daily average concentrations and standard deviations are given in Fig. 1a. As numerous factors such as traffic density, meteorological, and human activities could affect the diurnal cycle of VOC pollutants, the characteristics of diurnal variations could also reflect the sources, transportation, and chemical reaction of ambient VOCs (Lyu et al. 2016). Overall diurnal trend was similar during the sampling period and was consistent with patterns reported in literature (Kumar et al. 2018; Menchaca-Torre et al. 2015). In detail, ambient VOCs showed the highest concentrations in morning peak ($8:00 – 9:00$) and gradually decline to the lowest in midnight ($23:00 – 24:00$) with an obvious rebound in the afternoon ($15:00 – 16:00$). Generally, a combination of lower boundary layer height and release of VOCs from heavy traffic were the major reasons for the higher levels of VOCs in the morning peak hours (Garzón et al. 2015). In contrast, increased dispersion and dilution of the pollutants due to elevation of planetary boundary layer and the natural degradation of VOCs during nighttime jointly lead to the lowering of VOC levels in midnight (Menchaca-Torre et al. 2015).

Alkanes and aromatics followed the diurnal cycles which also showed good correlations with vehicle density reported in Li et al. (2017) in Xi'an. OVOCs did not show peaks in the morning but had dramatically high concentrations in afternoon and evening peak ($19:00 – 20:00$). This is because OVOCs could be formed by the high photochemical reactions of hydrocarbons with OH and NO_3 radicals during afternoon which could cumulate to evening (Sadanaga et al. 2019). While as the short life of OVOCs, the concentrations of OVOCs decreased significantly in midnight (Louie et al. 2013). Halocarbon did not follow the diurnal trends either but showed consistent concentrations during 1 day, which was probable because of the low reactivity in photochemical reactions and the less variable emission sources (Kumar et al. 2018).

As shown in Fig. 1, the daily average VOC concentrations both showed relative high levels in Saturday and Monday. A previous study indicated that the vehicle count at South 2nd Ring Road (close to the sampling site) was extremely high on weekend and Monday, which would dominate the daily variation during the campaign (Li et al. 2017). During weekend, citizens usually would like more activities (i.e., shopping and gathering) which will

Table 1 Composition of VOCs in different sampling time periods

VOC species	8:00–9:00		15:00–16:00		19:00–20:00		23:00–24:00			
	AVG	SD	AVG	SD	AVG	SD	AVG	SD	TAVG	TSD
Alkyne	3.79	3.72	0.99	0.50	1.67	2.10	0.76	0.30	1.80	2.41
Acetylene	3.79	3.72	0.99	0.50	1.67	2.10	0.76	0.30	1.80	2.41
Alkene	3.82	2.43	2.90	1.63	3.02	1.91	1.82	1.68	2.89	2.58
Ethylene	2.18	1.38	0.66	0.24	0.92	0.54	0.81	0.33	1.14	0.97
Propylene	0.34	0.14	0.24	0.11	0.24	0.10	0.24	0.13	0.27	0.13
1-Butene	0.35	0.38	0.35	0.21	0.35	0.20	0.44	0.77	0.37	0.44
Trans-2-butene	0.03	0.04	0.08	0.05	0.07	0.09	0.05	0.12	0.06	0.08
Cis-2-butene	0.02	0.03	0.05	0.06	0.06	0.07	0.02	0.04	0.04	0.05
1-Pentene	0.03	0.03	0.02	0.03	0.03	0.05	0.01	0.02	0.02	0.03
Isoprene	0.84	0.40	1.48	0.88	1.24	0.69	0.20	0.13	0.94	0.76
Trans-2-pentene	0.02	0.02	0.02	0.03	0.04	0.03	0.01	0.02	0.03	0.03
Cis-2-pentene	0.01	0.01	<DL	0.01	0.01	0.02	<DL	<DL	0.01	0.01
1-Hexene	<DL	<DL	<DL	<DL	<DL	<DL	<DL	<DL	<DL	<DL
1,3-Butadiene	<DL	<DL	<DL	<DL	0.04	0.12	0.03	0.10	0.02	0.08
Alkane	13.87	9.89	12.88	15.31	10.74	9.48	8.01	6.61	11.38	12.35
Ethane	3.09	1.16	1.83	1.16	1.36	0.78	1.62	0.79	1.97	1.17
Propane	1.50	0.48	1.31	0.95	0.97	0.56	1.02	0.51	1.20	0.67
Isobutane	1.14	0.93	1.66	2.17	3.02	3.49	1.07	1.55	1.72	2.31
n-Butane	1.71	1.34	1.64	2.02	1.98	2.68	1.25	1.10	1.65	1.85
Isopentane	3.00	3.08	2.18	2.21	1.14	0.29	1.17	1.04	1.87	2.06
n-Pentane	0.60	0.33	1.63	3.57	0.41	0.14	0.53	0.60	0.79	1.83
2,2-Dimethylbutane	0.02	0.02	0.01	0.02	0.01	0.02	<DL	0.01	0.01	0.02
Cyclopentane	0.06	0.04	0.08	0.11	0.05	0.07	0.02	0.02	0.05	0.07
2,3-Dimethylbutane	0.05	0.04	0.04	0.05	0.01	0.02	0.01	0.01	0.03	0.04
2-Methylpentane	0.23	0.12	0.20	0.26	0.17	0.11	0.10	0.06	0.18	0.16
3-Methylpentane	0.18	0.09	0.20	0.27	0.17	0.13	0.10	0.08	0.17	0.16
n-Hexane	0.97	1.53	0.78	1.21	0.33	0.31	0.28	0.33	0.59	1.01
Methylcyclopentane	0.06	0.03	0.06	0.07	0.05	0.04	0.02	0.02	0.05	0.05
2,4-Dimethylpentane	<DL	0.01	0.01	0.02	0.01	0.02	<DL	<DL	0.01	0.01
Cyclohexane	0.59	0.18	0.77	0.58	0.51	0.14	0.53	0.16	0.60	0.33
2-Methylhexane	0.04	0.03	0.03	0.05	0.04	0.04	<DL	<DL	0.02	0.04
2,3-Dimethylpentane	<DL	0.01	0.01	0.02	0.02	0.03	<DL	<DL	0.01	0.02
3-Methylhexane	0.05	0.03	0.04	0.06	0.04	0.04	0.02	0.02	0.04	0.04
2,2,4-Trimethylpentane	0.06	0.05	0.04	0.03	0.04	0.03	0.03	0.03	0.04	0.04
n-Heptane	0.19	0.19	0.09	0.08	0.11	0.11	0.09	0.09	0.12	0.13
Methylcyclohexane	0.06	0.03	0.07	0.10	0.09	0.14	0.03	0.03	0.06	0.09
2,3,4-Trimethylpentane	<DL	<DL	<DL	<DL	<DL	<DL	<DL	<DL	<DL	<DL
2-Methylheptane	0.01	0.01	<DL	0.01	0.01	0.02	<DL	0.01	0.01	0.01
3-Methylheptane	0.01	0.01	0.01	0.02	0.01	0.01	0.01	0.02	0.01	0.01
n-Octane	0.06	0.04	0.04	0.04	0.05	0.04	0.02	0.03	0.04	0.04
n-Nonane	0.05	0.03	0.02	0.02	0.04	0.03	0.02	0.02	0.03	0.03
n-Decane	0.04	0.02	0.05	0.09	0.04	0.02	0.03	0.02	0.04	0.05
n-Undecane	0.04	0.04	0.03	0.05	0.05	0.13	0.02	0.03	0.04	0.07
n-Dodecane	0.05	0.05	0.03	0.06	0.02	0.03	0.02	0.04	0.03	0.04
Benzene series	3.65	2.98	3.27	5.14	2.58	1.42	2.07	1.87	2.89	3.50
Benzene	1.07	1.50	0.46	0.50	0.37	0.28	0.58	0.95	0.62	0.94
Toluene	0.98	0.42	1.13	1.66	0.76	0.29	0.56	0.30	0.86	0.88
Ethylbenzene	0.29	0.17	0.31	0.57	0.30	0.17	0.17	0.10	0.27	0.31
m/p-Xylene	0.66	0.43	0.72	1.29	0.64	0.35	0.41	0.27	0.61	0.70
Styrene	0.15	0.16	0.20	0.42	0.07	0.05	0.06	0.04	0.12	0.23
o-Xylene	0.29	0.19	0.31	0.56	0.27	0.14	0.17	0.09	0.26	0.30
Isopropylbenzene	0.01	0.01	0.01	0.01	0.01	0.01	<DL	<DL	0.01	0.01
n-Propylbenzene	0.01	0.01	0.01	0.01	0.01	0.01	0.01	0.01	0.01	0.01
m-Ethyltoluene	0.04	0.02	0.02	0.02	0.03	0.02	0.03	0.02	0.03	0.02
p-Ethyltoluene	0.02	0.01	0.01	0.01	0.02	0.01	0.01	0.01	0.01	0.01
1,3,5-Trimethylbenzene	0.02	0.01	0.02	0.01	0.02	0.01	0.01	0.01	0.02	0.01
o-Ethyltoluene	0.02	0.01	0.01	0.01	0.01	0.01	0.01	0.01	0.01	0.01
1,2,4-Trimethylbenzene	0.06	0.03	0.04	0.03	0.05	0.04	0.04	0.03	0.05	0.03
1,2,3-Trimethylbenzene	0.02	0.01	0.01	0.01	0.01	0.01	0.01	0.01	0.01	0.01
m-Diethylbenzene	<DL	<DL	<DL	0.01	<DL	0.01	<DL	0.01	<DL	0.01
p-Diethylbenzene	<DL	0.01	<DL	0.01	<DL	0.01	<DL	0.01	<DL	0.01
Halohydrocarbon	8.79	7.65	8.58	6.66	7.19	5.03	4.92	2.33	7.37	7.27
Freon-12	0.63	0.06	0.62	0.05	0.67	0.10	0.61	0.07	0.63	0.07

Table 1 (continued)

VOC species	8:00–9:00		15:00–16:00		19:00–20:00		23:00–24:00			
	AVG	SD	AVG	SD	AVG	SD	AVG	SD	TAVG	TSD
Chloromethane	1.16	0.47	1.00	0.25	1.03	0.19	1.01	0.17	1.05	0.29
Freon-114	0.02	<DL	0.02	0.01	0.03	0.01	0.03	0.01	0.03	0.01
Vinyl chloride	0.04	0.04	0.03	0.05	0.02	0.04	0.02	0.02	0.03	0.04
Bromomethane	0.01	0.01	0.01	0.01	0.01	0.01	<DL	0.01	0.01	0.01
Chloroethane	0.05	0.04	0.04	0.04	0.04	0.05	0.02	0.03	0.04	0.04
Vinyl bromide	<DL	<DL	<DL	<DL	<DL	<DL	<DL	<DL	<DL	<DL
Freon-11	1.81	2.09	1.82	2.06	0.69	0.52	0.99	0.80	1.33	1.57
1,1-Dichloroethene	<DL	<DL	<DL	<DL	<DL	0.01	<DL	<DL	<DL	0.01
Methylene chloride	1.70	0.70	3.02	3.01	1.49	1.01	0.81	0.46	1.75	1.78
Allyl chloride	<DL	<DL	<DL	<DL	<DL	<DL	<DL	<DL	<DL	<DL
Freon-113	0.10	0.02	0.10	0.02	0.13	0.11	0.09	0.01	0.10	0.06
Trans-1,2-dichloroethene	0.01	0.02	<DL	0.01	<DL	0.01	<DL	<DL	<DL	0.01
1,1-Dichloroethane	0.19	0.27	0.14	0.15	0.11	0.09	0.04	0.05	0.12	0.17
Cis-1,2-dichloroethylene	<DL	<DL	<DL	<DL	<DL	<DL	<DL	<DL	<DL	<DL
Chloroform	1.42	2.99	0.41	0.23	0.33	0.18	0.27	0.21	0.61	1.53
1,2-Dichloroethane	0.87	0.40	0.76	0.39	1.47	1.43	0.60	0.28	0.93	0.83
1,1,1-Trichloroethane	<DL	<DL	<DL	<DL	<DL	<DL	<DL	<DL	<DL	<DL
Carbon tetrachloride	0.18	0.04	0.16	0.04	0.28	0.46	0.13	0.06	0.19	0.23
1,2-Dichloropropane	0.28	0.17	0.20	0.14	0.59	0.50	0.16	0.06	0.31	0.32
Bromodichloromethane	<DL	<DL	<DL	<DL	<DL	<DL	<DL	<DL	<DL	<DL
Trichloroethylene	0.05	0.12	0.01	0.02	0.01	0.04	<DL	0.02	0.02	0.07
Cis-1,3-dichloropropene	0.01	0.03	0.01	0.02	0.06	0.07	<DL	<DL	0.02	0.04
Trans-1,3-dichloropropene	<DL	<DL	<DL	<DL	<DL	<DL	<DL	<DL	<DL	<DL
1,1,2-Trichloroethane	0.02	0.02	0.02	0.03	0.05	0.09	<DL	0.01	0.02	0.05
Dibromochloromethane	<DL	<DL	<DL	<DL	<DL	<DL	<DL	<DL	<DL	<DL
1,2-Dibromoethane	<DL	<DL	<DL	<DL	<DL	<DL	<DL	<DL	<DL	<DL
Tetrachloroethylene	0.04	0.03	0.04	0.04	0.02	0.02	0.01	0.01	0.03	0.03
Chlorobenzene	0.11	0.04	0.14	0.05	0.09	0.02	0.08	0.02	0.11	0.04
Bromoform	<DL	<DL	<DL	<DL	<DL	<DL	<DL	<DL	<DL	<DL
1,1,2,2-Tetrachloroethane	<DL	<DL	<DL	<DL	<DL	<DL	<DL	<DL	<DL	<DL
1,3-Dichlorobenzene	<DL	<DL	<DL	<DL	<DL	<DL	<DL	<DL	<DL	<DL
Benzyl chloride	<DL	<DL	<DL	<DL	<DL	<DL	<DL	<DL	<DL	<DL
1,4-Dichlorobenzene	0.03	0.04	0.01	0.02	0.01	0.02	<DL	0.01	0.01	0.03
1,2-Dichlorobenzene	<DL	<DL	<DL	<DL	<DL	<DL	<DL	<DL	<DL	<DL
1,2,4-Trichlorobenzene	<DL	0.01	<DL	<DL	0.01	0.02	<DL	<DL	<DL	0.01
Hexachloro-1,3-butadiene	0.04	0.03	0.02	0.02	0.04	0.02	0.03	0.02	0.03	0.02
Oxygenated VOCs	15.4	13.2	17.3	14.0	20.5	23.6	10.5	12.3	15.9	17.3
Acetone	11.9	8.67	14.0	8.50	14.0	9.53	7.81	6.19	11.9	8.44
Isopropyl alcohol	1.62	1.35	1.57	1.85	1.92	1.99	1.27	1.54	1.60	1.66
Methyl tert-butyl ether	0.25	0.17	0.18	0.11	0.24	0.13	0.14	0.09	0.20	0.13
Vinyl acetate	0.53	1.12	0.39	1.02	2.02	4.89	0.81	2.80	0.94	2.90
Methyl ethyl ketone	1.04	1.88	0.57	1.12	2.01	6.31	0.50	1.74	1.03	3.39
Ethyl acetate	<DL	<DL	0.55	1.46	0.22	0.76	<DL	<DL	0.19	0.83
Tetrahydrofuran	<DL	<DL	<DL	<DL	<DL	<DL	<DL	<DL	<DL	<DL
1,4-Dioxane	<DL	<DL	<DL	<DL	<DL	<DL	<DL	<DL	<DL	<DL
Methyl isobutyl ketone	<DL	<DL	<DL	<DL	<DL	<DL	<DL	<DL	<DL	<DL
Methyl butyl ketone	<DL	<DL	<DL	<DL	<DL	<DL	<DL	<DL	<DL	<DL
Others	0.33	0.23	0.29	0.14	0.40	0.55	0.34	0.45	0.34	0.37
Carbon disulfide	0.33	0.23	0.29	0.14	0.40	0.55	0.34	0.45	0.34	0.37
∑VOCs	49.6	40.1	46.2	43.4	46.0	44.1	28.4	25.6	42.6	45.8

AVG denotes average value

SD denotes standard deviation

TAVG denotes total average VOCs per day

TSD denotes total standard deviation for daily average VOCs

increase the burden of road traffic (Xu et al. 2018; Zou et al. 2019), while for Monday, there will be generally traffic jams at this road due to many local reasons. In addition, this could also explain the extremely high concentrations in two Monday (17th and 24th July, 2018) among the 10 weekdays in the campaign.

Fig. 1 **a** Daily variations of TVOC concentrations and the main compositions. **b** Daily variations of concentrations of trace gas (1,2,3,4 in *x*-axis denotes 4 sampling periods in each day, 1 for morning period 8:00–9:00, 2 for afternoon period 15:00–16:00, 3 for evening period 18:00–19:00, 4 for night period 23:00–24:00)
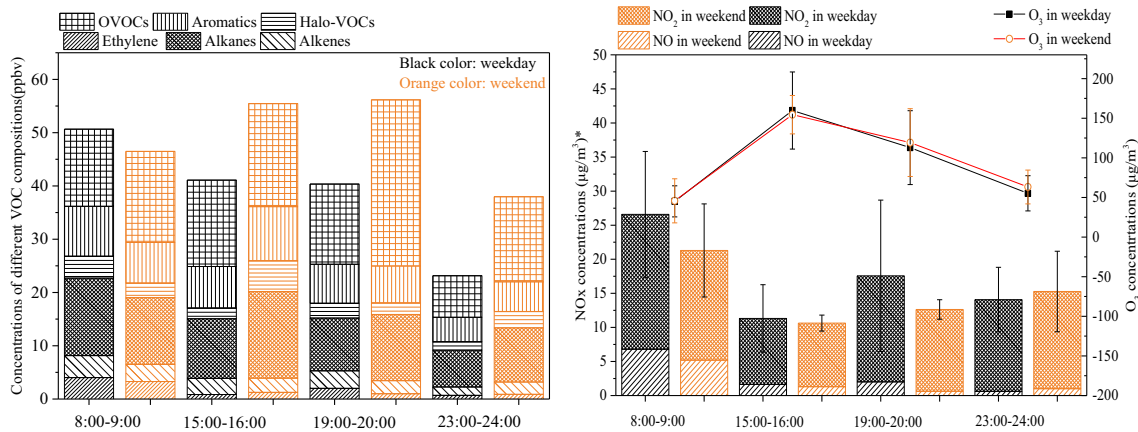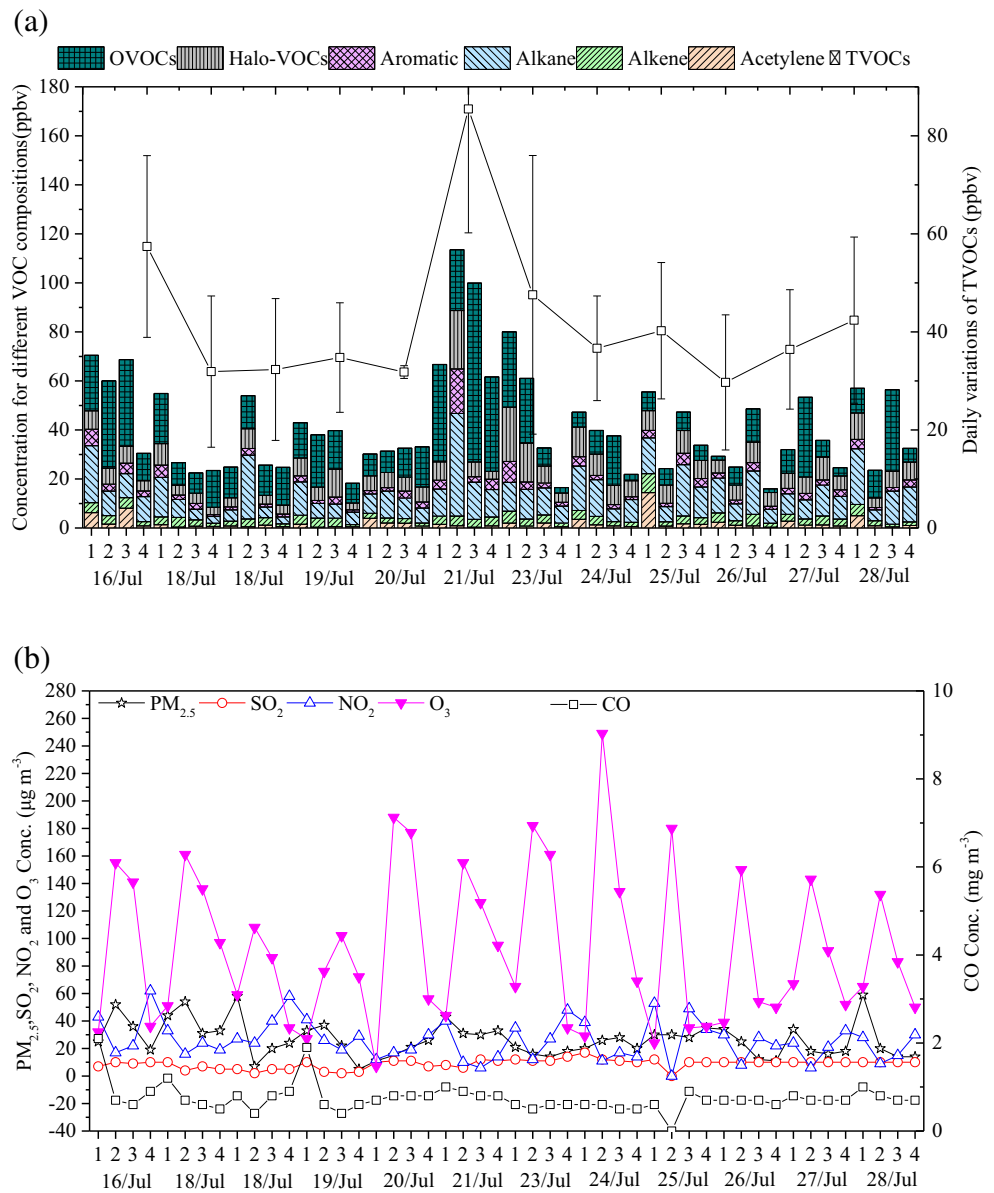
Fig. 2 Comparison of concentration of VOCs and gaseous pollutants between weekday and weekend

Table 2 Correlations between selected VOC individuals

	Isopentane	Benzene	Toluene	Ethylbenzene	m/p-Xylene	Isoprene	Chloromethane
Isopentane	1						
Benzene	0.30	1					
Toluene	0.66	0.61	1				
Ethylbenzene	0.22	0.39	0.73	1			
m/p-Xylene	0.25	0.39	0.70	0.99	1		
Isoprene	0.17	− 0.01	0.02	0.12	0.15	1	
Chloromethane	− 0.09	0.52	0.10	0.03	0.02	− 0.16	1

Concentrations of trace gaseous pollutants during the sampling period are listed in Fig. 1b. The data showed that PM$_{2.5}$ ranged from 5 to 89 μg m^{-3} (averagely 28.8 μg m^{-3}) which

led a favorable weather condition for ozone generation. SO$_2$ concentrations were quite stable that very small diurnal variation was observed. The relatively low concentrations of SO$_2$
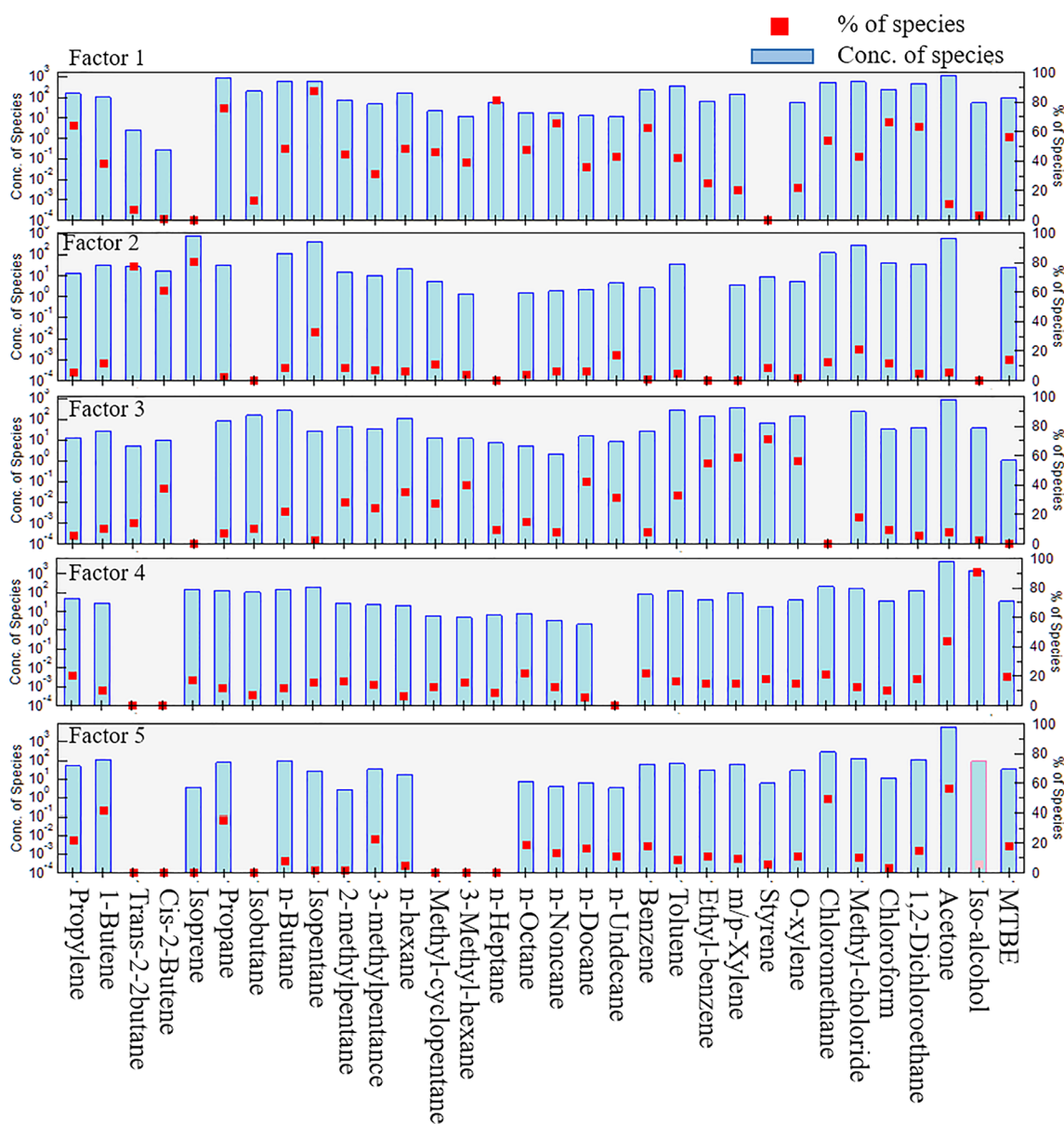
Fig. 3 Characters of 5 factors analyzed by PMF

Fig. 4 Source apportionment results from PMF
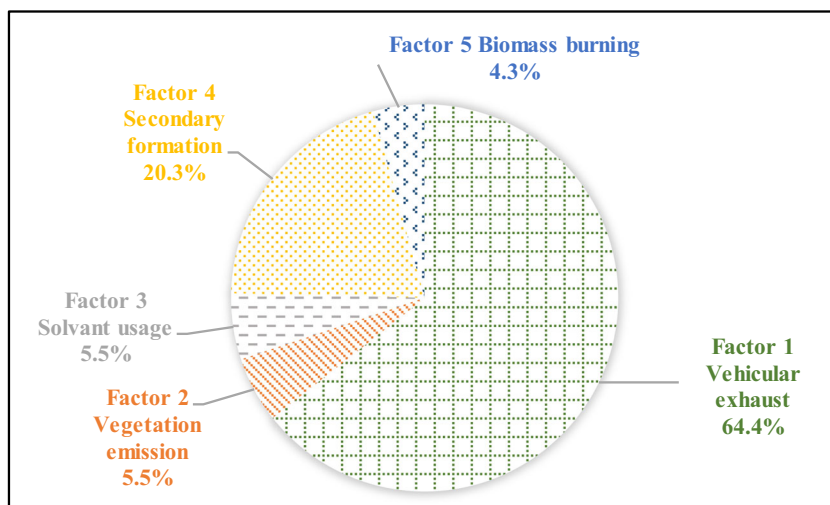
(9.2 ± 2.9 µg m^{-3}) indicated that coal combustion source was weak for this sampling site during the study. Comparably, NO_2 showed much high concentrations (25.3 ± 13.2 µg m^{-3}) than SO_2, referring that vehicular emissions showed stronger impacts to this sampling site. CO, generally derived from local sources, showed a descending order from morning to midnight, was inferred to be mainly affected by traffic emissions as well. NO_2 concentration showed obvious diurnal variations that a significant low peak was observed during the afternoon period. O_3 was the major pollutant during the sampling period with average concentration of 95.3 ± 55.4 µg m^{-3}, and even exceeded the national standard (160 µg m^{-3}, GB3095-2012) in afternoon period. The diurnal variation pattern of O_3 was contrary to NO_2 that the peak concentration happened in afternoon. Similar patterns were also observed in previous studies and a probable explanation was that the generation of O_3 from photochemical reactions would consume NO_2 (Feng et al. 2016; Tan et al. 2018).

To further detect the difference of VOCs between weekday and weekend, the comparison of concentration of VOCs and gaseous pollutants between weekday and weekend is done and shown in Fig. 2. The average VOC concentrations on weekend were statistically significantly higher than those over weekdays ($p < 0.05$). For the diurnal patterns, weekend showed much higher in the afternoon, night, and midnight periods but slightly lower VOC level in the morning. It is because most citizens were out of duty thus morning peak was weaker than weekdays. It has been reported that road traffic in weekend was much busier than weekdays especially in midnight which were even twice of weekdays (Li et al. 2017). This phenomenon was also observed in many literatures and commonly attributed the high VOC level on weekend to vehicle exhaust (Liu et al. 2016; Song et al. 2007; Warneke et al. 2013; Zhang et al. 2012). A further insight of VOC profiles on weekdays and weekend, higher alkanes (i.e., isopentane) on weekend also proved that traffic dominated the

Fig. 5 Time series variations of OFP during sampling period (MIR method) (1,2,3,4 in x-axis denotes 4 sampling periods in each day, 1 for morning period 8:00–9:00, 2 for afternoon period 15:00–16:00, 3 for evening period 18:00–19:00, 4 for night period 23:00–24:00)
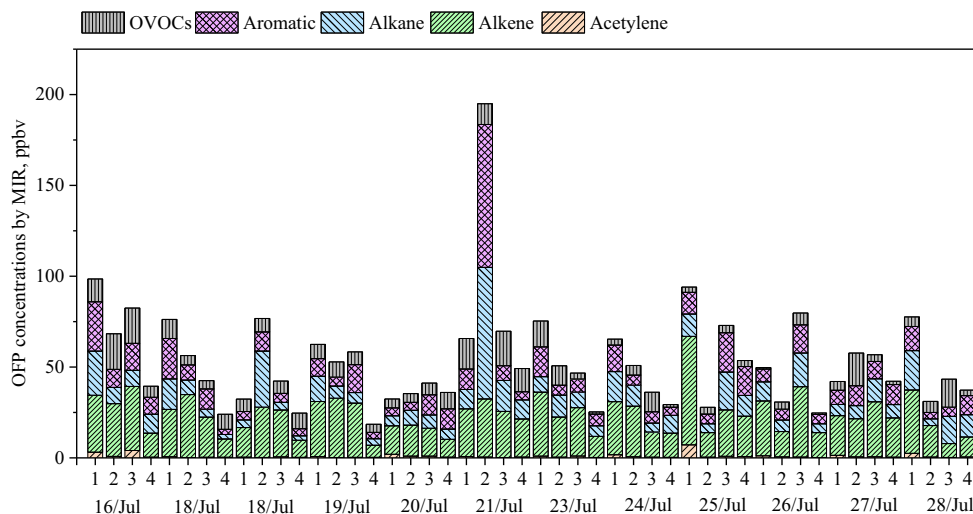
Table 3 Top ten contributors to OFP in different time periods during sampling time (ppbv)

8:00–9:00		15:00–16:00		19:00–20:00		23:00–24:00	
Ethylene	16.2	Isopentane	24.6	Isoprene	11.3	Ethylene	5.99
Isopropyl alcohol	7.65	Isoprene	13.4	Acetone	7.86	Acetone	4.37
1-Hexene	6.67	Acetone	7.84	Ethylene	6.82	m/p-Xylene	3.03
Methylcyclohexane	4.92	m/p-Xylene	5.33	m/p-Xylene	4.76	1-Butene	2.32
n-Butane	4.14	Ethylene	4.88	Isobutane	3.65	Propylene	2.28
m/p-Xylene	3.23	Isobutane	4.46	Propylene	2.28	Isoprene	1.85
p-Ethyltoluene	2.66	Toluene	3.06	Toluene	2.06	Isopentane	1.61
2,2,4-Trimethylpentane	1.90	Propylene	2.21	n-Butane	2.02	Toluene	1.51
Isoprene	1.89	o-Xylene	2.00	1-Butene	1.86	Isobutane	1.29
Toluene	1.86	1-Butene	1.87	o-Xylene	1.75	n-Butane	1.27
Subtotal of 10 OFP species	51.1		69.7		44.3		25.5
Total OFP	64.3		82.7		56.0		33.7
Ratio of subtotal OFP to total OFP	79%		84%		79%		76%

high VOCs on weekend. Another interesting finding was that the OVOC concentrations on weekend were much higher than those on weekdays ($p < 0.05$); however, it does not lead to significant higher O_3 concentrations on weekend than weekdays ($p > 0.05$).

VOC source apportionment

Source identification could be realized by many methods (i.e., species abundance, diagnostic ratios, and correlations) which could facilitate the further source apportionment (Liu et al. 2008; Parra et al. 2009; Kumar et al. 2018; Singh et al. 2016). As shown in Table S5, isopentane and acetone were abundant in morning and afternoon period, respectively, indicating vehicle emission and secondary formation were two main potential sources. Good correlations between isopentane/toluene (0.66) and toluene/benzene (0.61) (Table 2) supported the conclusion above, indicating a certain contribution from vehicle emissions (Li et al. 2017). To further

examine the importance of vehicle emission and other sources, the ratios of i-pentane to n-pentane and toluene to benzene were calculated using the linear regression method and compared with the two VOC sources (Wang et al. 2013) (Fig. S3). The calculated ratios for i-pentane/n-pentane and toluene/benzene both fell between the lines for vehicular emission obtained in tunnel study (Cui et al. 2018; Hwa et al. 2002) and household coal combustion (Liu et al. 2008), but were much close to coal combustion zone, indicating that the ambient VOCs in this study were majority affected by vehicular exhaust.

To further detect the contribution from different VOC sources, source apportionment was conducted by PMF which was described in the "Source apportionment model" section and Section S2. After running the PMF model, five factors were selected according to the resulted stable Q values and the characters are shown in Fig. 3. Factor 1 was distinguished by high percentages of C_3–C_6 alkane (especially isopentane) which are associated with unburned vehicular emissions

Fig. 6 Comparison of O_3 concentrations with OFP calculated by MIR and Prop-Equiv methods (1,2,3,4 in x-axis denotes 4 sampling periods in each day, 1 for morning period 8:00–9:00, 2 for afternoon period 15:00–16:00, 3 for evening period 18:00–19:00, 4 for night period 23:00–24:00)
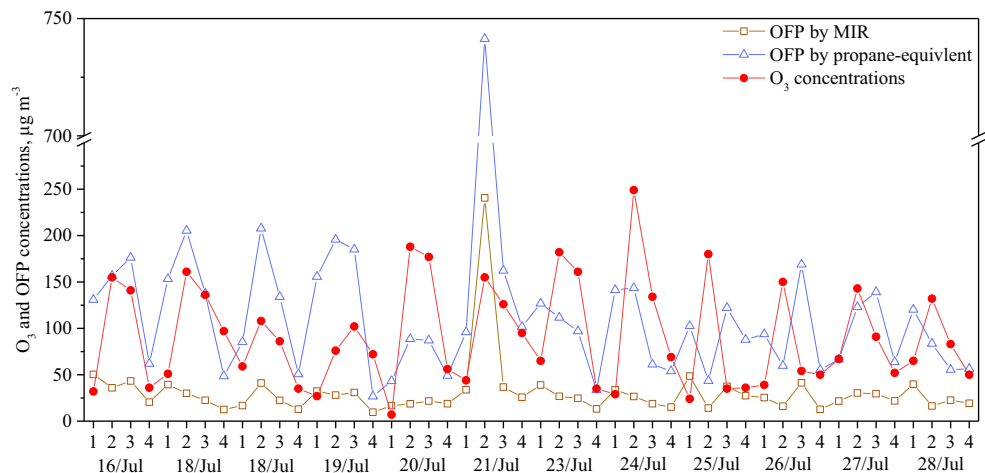
(Guo et al. 2004); additionally, toluene is usually related to vehicular emissions (Ho et al. 2009). Therefore, factor 1 could be considered as vehicular emission. The dramatically high peak of isoprene in source 2 indicated that the isoprene was mostly emitted by vegetation (Shao et al. 2016). Source 3 is associated with high percentages of toluene, ethylbenzene, and xylenes, with a certain amount of high-C-number alkanes. It is well known that these above mentioned aromatics can be emitted from solvent use (Borbon et al. 2002) Monod et al., 2001. Source 4 showed very low percentages of hydrocarbons but significantly high percentages of oxygenated VOCs (acetone, isopropyl, and alcohol), indicating that this source could be secondary formation in the atmosphere (Singh et al. 1994). Since chloromethane is normally considered as a typical tracer of biomass/biofuel burning (Liu et al. 2008), the high percentage of chloromethane and acetone, as well as certain percentages of short-chain alkenes and aromatics, indicating source 5 should be biomass burning (Wang et al. 2014).

Figure 4 presents the individual contribution of each source to the VOCs measured at the sampling site in summer Xi'an. Vehicular emission was the major source with contribution of 64.4% to ambient VOCs at this site, which was consistent with the discussion above. However, this proportion from vehicle-related emission was markedly higher when compared with source apportionment results in other megacities, such as Shanghai (25%) and Beijing (33%) (Li et al. 2018) Sheng et al., 2018. The high contribution from vehicle emission could be attributed to the heavy traffic near the sampling site. Secondary formation from photochemical reactions was the second largest source to the VOCs (20.3%) because of the favorable weather conditions (i.e., high temperature and strong sunlight). Vegetation emissions, solvent usage, and biomass burning all showed ~ 5% contributions to the ambient VOCs which were much weaker than the two main sources. In summary, located in the commercial and educational zone and far away from industries and suburb, the sampling site in this study was mainly influenced by vehicular emissions and secondary formation while contributions from solvent usage, biomass burning, and vegetation emissions were limited.

Ozone formation potential

Figure 5 shows the time series variations of OFP during sampling period by MIR method. Generally, the results showed that average OFP followed the sequence of alkenes > aromatics ≈ alkanes > OVOCs > alkyne. Alkenes were the largest contributor in OFP during the campaign which averagely accounts for 44.5% of total OFP. As the occupation of alkenes in TVOC was not great, the high OFP of alkenes was mainly due

to their high reactivity in photochemical reactions (Hui et al. 2018). Aromatics and alkanes showed comparable contributions to OFP (both ~ 19%), although the concentrations of alkanes were much higher than aromatics in the sampling site, the lower photochemical reaction activity limited their contributions to ozone formation (Carter 2009). OVOCs also showed fair contribution (15.1%) to total OFP of which acetone was the greatest individual contributor. The time series variations showed that the total OFP ranged from 18.5 to 195 ppbv in which a factor over 10 was observed. An unusual peak in 15:00–16:00 22nd July 2018 was observed; however, the OFP compositions were different. The dramatically high contribution from aromatics and alkanes deduced that this episode should be derived from heavy traffic emissions instead of photochemical reactions as the other compositions during afternoon periods.

OFP of individual VOC species also varied significantly. Table 3 lists the top ten VOC species from the OFP by MIR method. The top ten species contributed majority of the total OFPs with contributions from 76 to 84%. This indicated that the target VOC individuals would be very important in O_3 pollutant control. In detail, ethylene, isopentane, isoprene, acetone, m/p-xylene, and toluene showed higher photochemical reaction reactivity and contributed most of OFPs, which was similar with Hui et al. (2018). Of the top ten OFP contributors, ethylene was the largest composition in the morning and midnight periods while isopentane contributed over 30% the total OFP in afternoon. Ethylene and isopentane could both be emitted from combustion-related sources (i.e., coal combustion, biomass burning, and vehicle emission) (Shao et al. 2016; Song et al. 2019), but considering the source apportionment results in former section, vehicular emission is probably the largest contributor to these two species and consequently should be prior controlled in Xi'an. Isoprene, as a marker for biogenic VOCs, showed certain high OFPs in all periods (from 1.85 to 13.4 ppbv), indicating that biogenic VOCs could not be ignored in urban Xi'an city when controlling O_3 pollutants.

Comparison of measured O_3 concentrations with OFP calculated by MIR and Prop-Equiv methods is drawn in Fig. 6. Marked overestimation was observed for Prop-Equiv method compared with the measured ambient O_3 concentrations. As reported in literature, the ground-level O_3 could not be derived from both local photochemical reactions and regional transportation (Feng et al. 2016). The overestimation of OFP by Prop-Equiv method could be explained by the extremely high k_{OH}s in the calculation which were too ideal to happen in realistic atmosphere, while MIR method has considered multiple atmospheric conditions including temperature, NO_x concentrations, etc. (Carter 2009). Thus, it could be concluded that MIR method was more reasonable in evaluation of the OFPs in summer Xi'an.

Conclusion

Urban VOC profiles were measured using SUMMA canister method during 16th to 28th July 2018 with time resolution of 4 times per day and 1 h per time (8:00–9:00, 15:00–16:00, 19:00–20:00, and 23:00–24:00) in Xi'an, China. Eighty-six out of 106 species were detected with concentrations higher than MDLs and the TVOC levels ranged from 24.3 to 61.4 ppbv. Temporal variations showed decline concentrations from morning to midnight with an obvious rebound in afternoon. The vehicle density could explain the extremely high VOC concentrations during morning periods and also strong weekend effects on VOC concentrations ($p < 0.05$). However, the O_3 concentrations in weekend were not significantly higher than those over weekdays ($p > 0.05$). Isopentane variations indicated that vehicle emissions were dominant in the morning while acetone which was formed by photochemical reactions increased and cumulated in the afternoon and evening periods. The diagnostic ratios of i-pentane/n-pentane and toluene/benzene in this study were highly close to those reported in tunnel study which indicated that vehicular emissions were the largest source to the VOCs in this sampling site. PMF results confirmed that vehicular emission was the most important source to ambient VOCs (64.4%) followed by secondary formation (20.3%), while vegetation emission, solvent usage, and biomass burning showed comparable contributions (~ 5%). OFP results from MIR and Prop-Equiv showed that alkenes had the highest OFP followed by aromatics, alkanes, and OVOCs. A marked overestimation was observed in Prop-Equiv-based OFP calculation, resulting that MIR method was more reasonable and suitable for OFP evaluation in summer Xi'an. The results in this study indicated that vehicular emission has taken the place of industrial emission to be the major VOC source in summer Xi'an led by the deindustrialization policy. Vehicular emission and biogenic source should be priority controlled when making regional ozone control policies.

References

An J, Wang J, Zhang Y, Zhu B (2017) Source apportionment of volatile organic compounds in an urban environment at the Yangtze River Delta, China. Arch Environ Contam Toxicol:335–348

Atkinson R, Arey J (2003) Atmospheric degradation of volatile organic compounds. Chem Rev 103:4605–4638

Borbon A, Locoge N, Veillerot M, Galloo JC, Guillermo R (2002) Characterisation of NMHCs in a French urban atmosphere: overview of the main sources. Sci Total Environ 292:177–191

Cai C, Geng F, Tie X, Yu Q, An J (2010) Characteristics and source apportionment of VOCs measured in Shanghai, China. Atmos Environ 44:5005–5014

Cao J, Shen Z, Chow JC, Watson JG, Lee S, Tie X, Ho K, Wang G, Han Y (2012) Winter and summer PM2.5 chemical compositions in fourteen Chinese cities. J Air Waste Manage 62:1214–1226

Carter, W. P., 2009. Carter W PL. Updated maximum incremental reactivity scale and hydrocarbon bin reactivities for regulatory applications. California Air Resources Board Contract 2009, 339

Cheng L, Wang S, Gong Z, Li H, Yang Q, Wang Y (2018) Regionalization based on spatial and seasonal variation in ground-level ozone concentrations across China. J Environ Sci 67:179–190

Cui L, Wang XL, Ho KF, Gao Y, Liu C, Hang Ho SS, Li HW, Lee SC, Wang XM, Jiang BQ, Huang Y, Chow JC, Watson JG, Chen L-W (2018) Decrease of VOC emissions from vehicular emissions in Hong Kong from 2003 to 2015: results from a tunnel study. Atmos Environ 177:64–74

Duan J, Tan J, Yang L, Wu S, Hao J (2008) Concentration, sources and ozone formation potential of volatile organic compounds (VOCs) during ozone episode in Beijing. Atmos Res 88:25–35

Feng T, Bei N, Huang RJ, Cao J, Zhang Q, Zhou W, Tie X, Liu S, Zhang T, Su X, Lei W, Molina LT, Li G (2016) Summertime ozone formation in Xi'an and surrounding areas, China. Atmos Chem Phys 16: 4323–4342

Garzón JP, Huertas JI, Magaña M, Huertas ME, Cárdenas B, Watanabe T, Maeda T, Wakamatsu S, Blanco S (2015) Volatile organic compounds in the atmosphere of Mexico City. Atmos Environ 119: 415–429

Guo H, Cheng HR, Ling ZH, Louie PKK, Ayoko GA (2011) Which emission sources are responsible for the volatile organic compounds in the atmosphere of Pearl River Delta? J Hazard Mater 188:116–124

Guo H, Lee SC, Chan LY, Li WM (2004) Risk assessment of exposure to volatile organic compounds in different indoor environments. Environmental Research 94 (1):57–66

Han D, Wang Z, Cheng J, Wang Q, Chen X, Wang H (2017) Volatile organic compounds (VOCs) during non-haze and haze days in Shanghai: characterization and secondary organic aerosol (SOA) formation. Environ Sci Pollut Res 24:18619–18629

Ho KF, Lee SC, Ho WK, Blake DR, Cheng Y, Li YS, Ho SSH, Fung K, Louie PKK, Park D (2009) Vehicular emission of volatile organic compounds (VOCs) from a tunnel study in Hong Kong. Atmos Chem Phys 9:7491–7504

Hoshi J-Y, Amano S, Sasaki Y, Korenaga T (2008) Investigation and estimation of emission sources of 54 volatile organic compounds in ambient air in Tokyo. Atmos Environ 42:2383–2393

Huang Y, Ling ZH, Lee SC, Ho SSH, Cao JJ, Blake DR, Cheng Y, Lai SC, Ho KF, Gao Y, Cui L, Louie PKK (2015) Characterization of volatile organic compounds at a roadside environment in Hong Kong: an investigation of influences after air pollution control strategies. Atmos Environ 122:809–818

Hui L, Liu X, Tan Q, Feng M, An J, Qu Y, Zhang Y, Jiang M (2018) Characteristics, source apportionment and contribution of VOCs to ozone formation in Wuhan, Central China. Atmos Environ 192: 55–71

Hwa M-Y, Hsieh C-C, Wu T-C, Chang L-FW (2002) Real-world vehicle emissions and VOCs profile in the Taipei tunnel located at Taiwan Taipei area. Atmos Environ 36:1993–2002

Kampa M, Castanas E (2008) Human health effects of air pollution. Environ Pollut 151:362–367

Kountouriotis A, Aleiferis PG, Charalambides AG (2014) Numerical investigation of VOC levels in the area of petrol stations. Sci Total Environ 470-471:1205–1224

Kumar A, Singh D, Anandam K, Kumar K, Jain VK (2017) Dynamic interaction of trace gases (VOCs, ozone, and NOx) in the rural

atmosphere of sub-tropical India. Air Qual Atmos Health 10:885–896

Kumar A, Singh D, Kumar K, Singh BB, Jain VK (2018) Distribution of VOCs in urban and rural atmospheres of subtropical India: temporal variation, source attribution, ratios, OFP and risk assessment. Sci Total Environ 613-614:492–501

Lee SC, Chiu MY, Ho KF, Zou SC, Wang X (2002) Volatile organic compounds (VOCs) in urban atmosphere of Hong Kong. Chemosphere 48:375–382

Li J, Xie SD, Zeng LM, Li LY, Li YQ, Wu RR (2015) Characterization of ambient volatile organic compounds and their sources in Beijing, before, during, and after Asia-Pacific Economic Cooperation China 2014. Atmos Chem Phys 15:7945–7959

Li B, Ho SSH, Xue Y, Huang Y, Wang L, Cheng Y, Dai W, Zhong H, Cao J, Lee S (2017) Characterizations of volatile organic compounds (VOCs) from vehicular emissions at roadside environment: the first comprehensive study in Northwestern China. Atmos Environ 161:1–12

Li N, He Q, Greenberg J, Guenther A, Li J, Cao J, Wang J, Liao H, Wang Q, Zhang Q (2018) Impacts of biogenic and anthropogenic emissions on summertime ozone formation in the Guanzhong Basin, China. Atmos Chem Phys 18:7489–7507

Li K, Jacob DJ, Liao H, Shen L, Zhang Q, Bates KH (2019) Anthropogenic drivers of 2013–2017 trends in summer surface ozone in China. Proc Natl Acad Sci U S A 116:422–427

Liu Y, Shao M, Fu L, Lu S, Zeng L, Tang D (2008) Source profiles of volatile organic compounds (VOCs) measured in China: part I. Atmos Environ 42:6247–6260

Liu Z, Li N, Wang N (2016) Characterization and source identification of ambient VOCs in Jinan, China. Air Qual Atmos Health 9:285–291

Louie PKK, Ho JWK, Tsang RCW, Blake DR, Lau AKH, Yu JZ, Yuan Z, Wang X, Shao M, Zhong L (2013) VOCs and OVOCs distribution and control policy implications in Pearl River Delta region, China. Atmos Environ 76:125–135

Lyu X, Chen N, Guo H, Zhang WH, Wang N, Wang Y, Liu M (2016) Ambient volatile organic compounds and their effect on ozone production in Wuhan, central China. Sci Total Environ 541:200–209

Menchaca-Torre HL, Mercado-Hernández R, Rodríguez-Rodríguez J, Mendoza-Domínguez A (2015) Diurnal and seasonal variations of carbonyls and their effect on ozone concentrations in the atmosphere of Monterrey, Mexico. J Air Waste Manage 65:500–510

Monod A, Sive BC, Avino P, Chen T, Blake DR, Sherwood Rowland F (2001) Monoaromatic compounds in ambient air of various cities: a focus on correlations between the xylenes and ethylbenzene. Atmos Environ 35:135–149

NBSC (2018) National Bureau of Statistics of China. http://data.stats.gov.cn/search.htm?s=2018%20GDP

Parra MA, Elustondo D, Bermejo R, Santamaría JM (2009) Ambient air levels of volatile organic compounds (VOC) and nitrogen dioxide (NO2) in a medium size city in northern Spain. Sci Total Environ 407:999–1009

Sadanaga Y, Ishiyama A, Takaji R, Matsuki A, Kato S, Sato K, Osada K, Bandow H (2019) Behavior of total peroxy and total organic nitrate concentrations at Suzu on the Noto Peninsula, Japan: long-range transport and local photochemical production. Atmos Environ 196:20–26

Shao P, An J, Xin J, Wu F, Wang J, Ji D, Wang Y (2016) Source apportionment of VOCs and the contribution to photochemical ozone formation during summer in the typical industrial area in the Yangtze River Delta, China. Atmos Res 176-177:64–74

Shen Z, Arimoto R, Cao J, Zhang R, Li X, Du N, Okuda T, Nakao S, Tanaka S (2008) Seasonal variations and evidence for the effectiveness of pollution controls on water-soluble inorganic species in total suspended particulates and fine particulate matter from Xi'an, China. J Air Waste Manage 58:1560–1570

Shen Z, Cao J, Arimoto R, Han Z, Zhang R, Han Y, Liu S, Okuda T, Nakao S, Tanaka S (2009) Ionic composition of TSP and PM2.5 during dust storms and air pollution. Atmos Environ 43:2911–2918

Shen ZX, Cao JJ, Arimoto R, Han YM, Zhu CS, Tian J, Liu SX (2010) Chemical characteristics of fine particles (PM1) from Xi'an, China. Aeros Sci Technol 44(6):461–472

Shen ZX, Cao JJ, Liu SX, Zhu CS, Wang X, Zhang T, Xu HM, Hu TF (2011) Chemical composition of PM10 and PM2.5 collected at ground level and 100 meters during a strong winter-time pollution episode in Xi'an, China. J Air Waste Manage 61:1150–1159

Shen Z, Cao J, Zhang L, Zhang Q, Huang RJ, Liu S, Zhao Z, Zhu C, Lei Y, Xu H, Zheng C (2016) Retrieving historical ambient PM2.5 concentrations using existing visibility measurements in Xi'an, Northwest China. Atmos Environ 126:15–20

Sheng J, Zhao D, Ding D, Li X, Huang M, Gao Y, Quan J, Zhang Q (2018) Characterizing the level, photochemical reactivity, emission, and source contribution of the volatile organic compounds based on PTR-TOF-MS during winter haze period in Beijing, China. Atmos Res 212:54–63

Singh HB, O'Hara D, Herlth D, Sachse W, Blake DR, Bradshaw JD, Kanakidou M, Crutzen PJ (1994) Acetone in the atmosphere: distribution, sources, and sinks. J Geophys Res Atmos 99:1805–1819

Singh D, Kumar A, Kumar K, Singh B, Mina U, Singh BB, Jain VK (2016) Statistical modeling of O3, NOx, CO, PM2.5, VOCs and noise levels in commercial complex and associated health risk assessment in an academic institution. Sci Total Environ 572:586–594

Song Y, Shao M, Liu Y, Lu S, Kuster W, Goldan P, Xie S (2007) Source apportionment of ambient volatile organic compounds in Beijing. Environ Sci Technol 41:4348–4353

Song S-K, Shon Z-H, Kang Y-H, Kim K-H, Han S-B, Kang M, Bang J-H, Oh I (2019) Source apportionment of VOCs and their impact on air quality and health in the megacity of Seoul. Environ Pollut 247:763–774

SPBS (2017) http://www.shaanxitj.gov.cn/upload/2018/7/zk/indexce.htm. Shaanxi provincial bureau of statistics

Sun J, Wang J, Shen Z, Huang Y, Zhang Y, Niu X, Cao J, Zhang Q, Xu H, Zhang N, Li X (2019) Volatile organic compounds from residential solid fuel burning in Guanzhong Plain, China: source-related profiles and risks. Chemosphere 221:184–192

Tan Z, Lu K, Jiang M, Su R, Dong H, Zeng L, Xie S, Tan Q, Zhang Y (2018) Exploring ozone pollution in Chengdu, southwestern China: a case study from radical chemistry to O3-VOC-NOx sensitivity. Sci Total Environ 636:775–786

USEPA (1998) Photochemical assessment monitoring stations (PAMS) issue summary. Office of Air Quality Planning and Standards, Research Triangle Park, NC. http://www.epa.gov/ttnamti1/files/ambient/pams/pamsiss.pdf

Wang X, Shen ZX, Cao JJ, Zhang LM, Liu L, Li JJ, Liu SX, Sun YF (2012) Characteristics of surface ozone at an urban site of Xi'an in Northwest China. J Environ Monitor 14:116–126

Wang M, Shao M, Lu S-H, Yang Y-D, Chen W-T (2013) Evidence of coal combustion contribution to ambient VOCs during winter in Beijing. Chin Chem Lett 24:829–832

Wang H, Lou S, Huang C, Qiao L, Tang X, Chen C, Zeng L, Wang Q, Zhou M, Lu S, Yu X (2014) Source profiles of volatile organic compounds from biomass burning in Yangtze River Delta, China. Aerosol Air Qual Res 14:818–828

Wang T, Xue L, Brimblecombe P, Lam YF, Li L, Zhang L (2017) Ozone pollution in China: a review of concentrations, meteorological influences, chemical precursors, and effects. Sci Total Environ 575:1582–1596

Wang H, Xiang Z, Wang L, Jing S, Lou S, Tao S, Liu J, Yu M, Li L, Lin L, Chen Y, Wiedensohler A, Chen C (2018) Emissions of volatile organic compounds (VOCs) from cooking and their speciation: a case study for Shanghai with implications for China. Sci Total Environ 621:1300–1309

Warneke C, Gouw JA, Edwards PM, Holloway JS, Gilman JB, Kuster WC, Graus M, Atlas E, Blake D, Gentner DR, Goldstein AH, Harley RA, Alvarez S, Rappenglueck B, Trainer M, Parrish DD (2013) Photochemical aging of volatile organic compounds in the Los Angeles basin: weekday-weekend effect. J Geophys Res Atmos 118:5018–5028

Xu Y, Ying Q, Hu J, Gao Y, Yang Y, Wang D, Zhang H (2018) Spatial and temporal variations in criteria air pollutants in three typical terrain regions in Shaanxi, China, during 2015. Air Qual Atmos Health 11: 95–109

Xue Y, Ho SSH, Huang Y, Li B, Wang L, Dai W, Cao J, Lee S (2017) Source apportionment of VOCs and their impacts on surface ozone in an industry city of Baoji, Northwestern China. Sci Rep 7:9979

Yuan B, Liu Y, Shao M, Lu S, Streets DG (2010) Biomass burning contributions to ambient VOCs species at a receptor site in the Pearl River Delta (PRD), China. Environ Sci Technol 44:4577–4582

Yuan B, Hu W, Shao M, Wang M, Chen W, Lu S, Zeng L, Hu M (2013) VOC emissions, evolutions and contributions to SOA formation at a receptor site in eastern China. Atmos Chem Phys 13:8815–8832

Yurdakul S, Civan M, Kuntasal Ö, Doğan G, Pekey H, Tuncel G (2018) Temporal variations of VOC concentrations in Bursa atmosphere. Atmos Pollut Res 9:189–206

Zhang Y, Mu Y, Liu J, Mellouki A (2012) Levels, sources and health risks of carbonyls and BTEX in the ambient air of Beijing, China. J Environ Sci 24:124–130

Zhang Q, Shen Z, Cao J, Zhang R, Zhang L, Huang RJ, Zheng C, Wang L, Liu S, Xu H, Zheng C, Liu P (2015) Variations in PM2.5, TSP, BC, and trace gases (NO2, SO2, and O3) between haze and non-haze episodes in winter over Xi'an, China. Atmos Environ 112: 64–71

Zhang Z, Zhang Y, Wang X, Lü S, Huang Z, Huang X, Yang W, Wang Y, Zhang Q (2016) Spatiotemporal patterns and source implications of aromatic hydrocarbons at six rural sites across China's developed coastal regions. J Geophys Res Atmos 121:6669–6687

Zhang B-T, An X-X, Wang Q, Yan H, Liu B-X, Zhang D-W (2018) Temporal variation, spatial distribution, and reactivity characteristics of air VOCs in Beijing 2015. J Environ Sci 39:4400–4407

Zou Y, Deng XJ, Zhu D, Gong DC, Wang H, Li F, Tan HB, Deng T, Mai BR, Liu XT, Wang BG (2015) Characteristics of 1 year of observational data of VOCs, NOx and O3 at a suburban site in Guangzhou, China. Atmos Chem Phys 15:6625–6636

Zou Y, Charlesworth E, Yin C, Yan X, Deng X, Li F (2019) The weekday/weekend ozone differences induced by the emissions change during summer and autumn in Guangzhou, China. Atmos Environ 199: 114–126